Novel Compact wide-band EBG Structure based on Tapered 1-D Koch Fractal Patterns

Juan de Dios Ruiz, Félix L. Martínez and Juan Hinojosa

***Abstract*— This letter presents a novel electromagnetic band-gap (EBG) structure in microstrip technology based on non-uniform one-dimensional (1-D) Koch fractal patterns whose dimensions and period are modulated by a tapering function that significantly improves the width of the bandgap. This wide bandgap is achieved by maintaining the *r*/*a* (radius to period) ratio of the Koch fractal patterns larger than 0.5 in the whole structure. In the pass-band region, an improved flat response is obtained by tapering the dimensions of the Koch fractal patterns etched in the ground plane, together with the width of the microstrip line, with a Kaiser distribution which also modulates the periodicity of the fractals. A major consequence of this modulation of the periodicity of the pattern is that this structure is much more compact than a uniform conventional one.**

***Index Terms*— Electromagnetic band-gap (EBG), wideband, Koch fractal, periodic structures, microstrip structures.**

I. Introduction

As photonic band-gap materials (PBGs) in Optics [1], electromagnetic band-gap structures (EBGs) are periodic patterns that exhibit a band of frequencies in which the electromagnetic propagation is not allowed in the microwave range [2]. EBG structures have a wide range of applications in antennas, amplifiers, filters, microwave cavities, etc [3]-[8]. In microstrip technology, the EBG structure is obtained by creating a one-dimensional (1-D) periodic pattern etched in the ground plane with circular, sinusoidal, triangular, square or fractal shapes and *r*/*a* (radius/period) ratios lower than 0.5 [9]-[12]. Usually, at least 4-5 periods are needed to provide good bandgap characteristics, and therefore a large physical space is required for integrating the EBG into a system [3]. Often, wide bandgap characteristics together with a compact design are desirable, although difficult to achieve. The objective of this study is to propose a new fractal structure that significantly improves the compatibility of both requirements thanks to the appropriate tapering of the dimensions and periodicity of the fractals.

In order to achieve the goals outlined in the previous paragraph, a periodic pattern etched in the ground plane with *r*/*a* ratios higher than 0.5 is considered [13]. It is based on level-1 Koch fractal element geometries [14], [15], which have been obtained from a hexagonal shape. The introduction of 1-D Koch fractal electromagnetic band-gap (KFEBG) microstrip structures with *r*/*a* ratios higher than 0.5 increases significantly the width of the bandgap, in such a way that wide-band structures with forbidden electromagnetic propagation in a wide frequency range become possible [13]. However, their behavior in the pass-band has been found to be not optimal, due to the appearance of ripples in this region. In [16], it is shown that it is possible to improve the performance of the conventional EBG structures by applying a tapering function to the radius of the holes. However, until now this technique has not been applied to fractal EBG structures with *r*/*a* ratios higher than 0.5.

In this work, we apply for the first time a Kaiser tapering function to 1-D KFEBG microstrip structures in order to maintain wide-bandgap characteristics and at the same time improve the performance in the band-pass frequency region. In order to avoid that the decreasing *r*/*a* ratio would negatively affect the wide bandgap frequency range, we have decreased the distance *a* between periodic patterns in order to maintain *r*/*a* ratios higher than 0.5 in the whole device. In this way, a compact wide-band KFEBG structure is achieved with much wider forbidden frequency gap and better band-pass performance than the uniform conventional structures.

II. Tapered KFEBG Microstrip Structures with Kaiser Distribution

The upper *r*/*a* ratio boundary of the conventional 1-D EBG microstrip structure can be exceeded by using a new pattern based on Koch fractal curves [14]. For this purpose, the first Koch fractal iteration with a scale factor of 1/3 is applied to a hexagonal shape and two possible cell geometries are obtained (Fig. 1). Thus, by combining and etching these level-1 Koch fractal hexagonal cells in the ground plane, instead of circular holes, it is possible to achieve 1-D Koch fractal electromagnetic bandgap (KFEBG) microstrip structures with *r*/*a* ratios higher than 0.5, as in Fig. 1 [13]. The design parameters of the 1-D KFEBG microstrip structure are the same as the conventional EBG structure: the distance *a* between the centers of the Koch fractal hexagonal cells, the radius *r* of the circumference in which the fractal shape is inscribed (represented by circles in dashed line in Fig. 1), and the total number *N* of etched cells. The central frequency of

Manuscript received June 30, 2011. This work was supported by Ministerio de Educación y Ciencia of Spain (TEC2010-21520-C04-04/TCM).

Authors are with the Departmento de Electrónica y Tecnología de Computadoras, Universidad Politécnica de Cartagena, Cartagena (Murcia) 30202, Spain (e-mail: juan.hinojosa@upct.es).

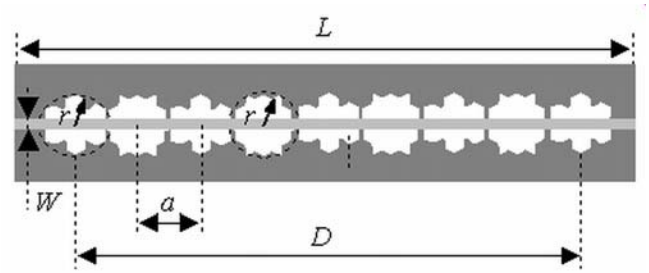

Fig. 1. 1-D KFEBG microstrip structure with nine level-1 Koch fractal hexagon cells etched in the ground plane (bottom plane). In the top plane, the width *W* of the conductor strip is constant along the structure.

the rejected band is obtained from $\lambda_g = 2a$, where λ_g is the guided wavelength in the unperturbed microstrip line. These level-1 Koch fractal hexagonal cells etched in the ground plane allow implementing *r*/*a* ratios lower than 0.5, as with non-fractal patterns, but also higher than 0.5.

Following previous works to improve the performance of conventional EBG microstrip structures by using tapered techniques [16], we have applied a Kaiser function to the radius of each level-1 Koch fractal hexagonal cell according to its position in the ground plane (Fig. 2). Among different tapering functions studied in [16], the Kaiser function provides the better compromise between side-lobe reduction and stop-band rejection level. The distance *a* between the centers of the Koch fractal hexagonal cells is kept constant. The radii distribution follows the next relationship

$$r_i = r_{max}\, T(z/L) \quad i = 0,1,\cdots \tag{1}$$

where r_i and r_{max} are the *i*-th and maximum Koch fractal hexagonal cell radii, respectively. z/L is the normalized longitudinal position in the circuit ($z = 0$ corresponds to the central point) and $T(z/L)$ is the tapering Kaiser function

$$T(z/L) = \frac{I_0\left(4\sqrt{1-2(z/L)^2}\right)}{I_0(4)} \tag{2}$$

where *L* is the length of the microstrip line and I_0 is the first-class modified Bessel function.

However, any change in the level-1 Koch fractal hexagonal cell radii (*a* being constant) affects the *r*/*a* ratio and, therefore, the frequency response of the device. Thus, we propose a second modification in order to maintain a constant *r*/*a* ratio. Instead of using a fixed period *a*, we modify it in proportion to the radii of the level-1 Koch fractal hexagonal cells so that the distance a_i between the centers of adjacent level-1 Koch fractal hexagonal cells follows the following function (Fig. 3)

$$a_i = r_{i-1}/C \quad i = 1,2,\cdots \tag{3}$$

where r_i is computed from (1) (r_0 corresponds to r_{max}) and *C* is a constant equal to the initial *r*/*a* ratio value of the non-tapered 1-D KFEBG microstrip structure (Fig. 1). Similarly, the Kaiser function and the varying period are applied to the width *W* of the conductor strip (Fig. 3(a)) in the top plane in order to reduce the impedance mismatch. Due to the reduction of the distance *D* between the centers of the two extreme Koch fractal cells, the circuit becomes more compact.

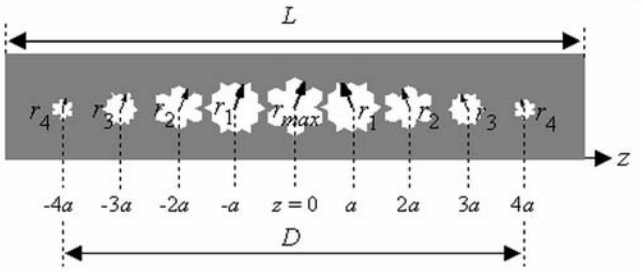

Fig. 2 Ground plane of the Kaiser-tapered 1-D KFEBG microstrip structure. In the top plane, the width *W* of the conductor strip is constant along the structure.

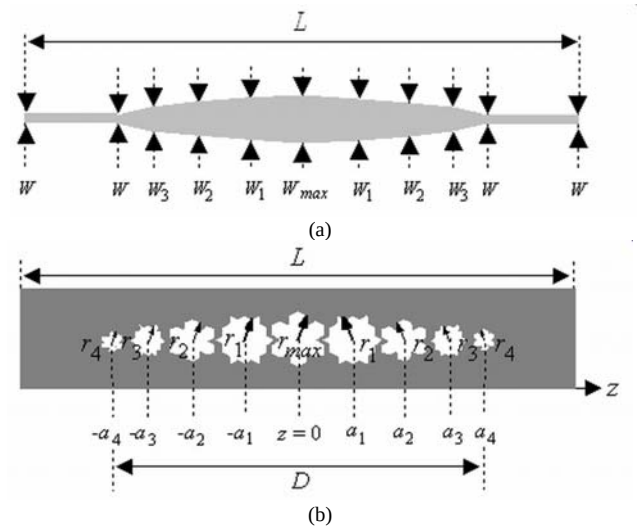

Fig. 3. Double Kaiser-tapered 1-D KFEBG microstrip structure with varying period. (a) Top plane. (b) Bottom plane.

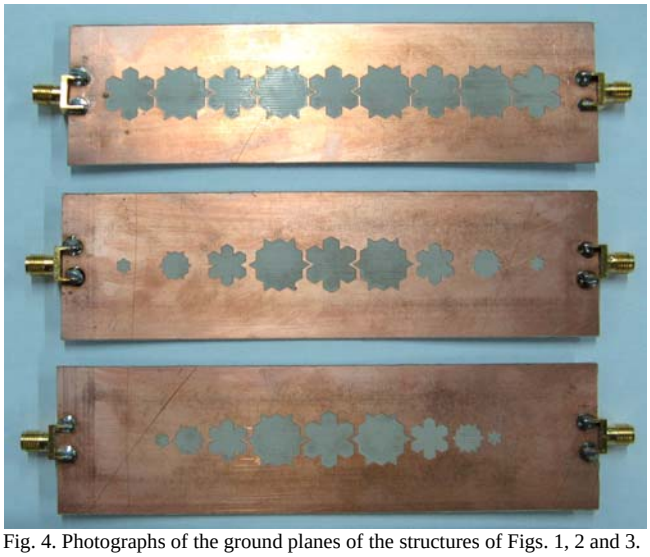

Fig. 4. Photographs of the ground planes of the structures of Figs. 1, 2 and 3.

TABLE I
DIMENSIONS OF THE DIFFERENT 1-D KFEBG MICROSTRIP STRUCTURES

Dimensions	Fig. 1	Fig. 2	Fig. 3
W	0.594 mm	0.594 mm	0.594 mm
a	14.1 mm	14.1 mm	—
r	7.755 mm	—	—
D	112.8 mm	112.8 mm	89.94 mm
r_{max}	—	7.755 mm	7.755 mm
W_{max}	—	—	2 mm
C	—	—	0.55

III. RESULTS

The 1-D KFEBG microstrip structures considered in Fig. 1 to Fig. 3 have been simulated and measured with the HFSS simulator and the Agilent 5071B vector network analyzer (VNA), respectively. The different 1-D KFEBG microstrip structures were fabricated by means of the numerical milling machine LPKF S62 (Fig. 4). The measurement system was calibrated from 300 kHz to 8 GHz.

The structure of Fig. 1 has been designed with the purpose to have an operation frequency of 4.2 GHz with the periodic value $a = 14.1$ mm and a radius to period ratio $r/a = 0.55$. The number of etched level-1 Koch fractal hexagonal cells has been set to N = 9 as in [9], [10] and the length of the microstrip line has been fixed to L = 141 mm. Arlon AD1000

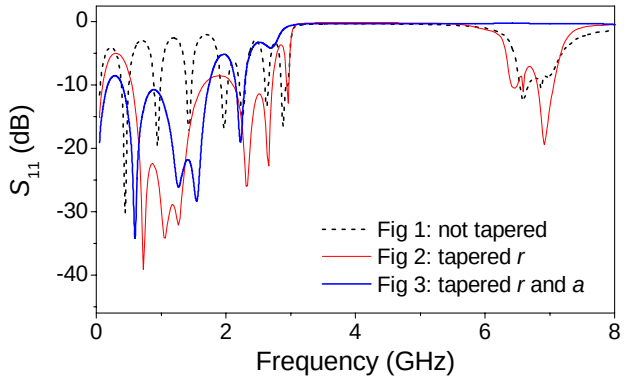

(a)

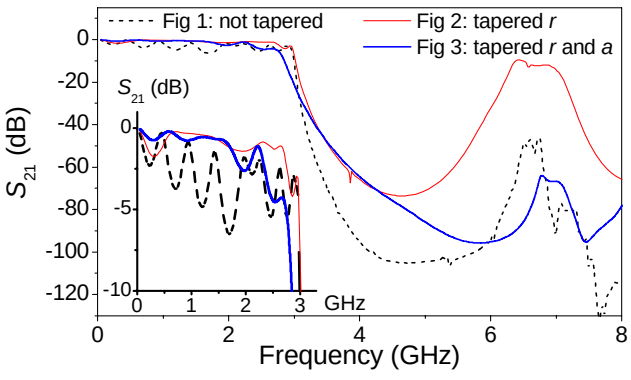

(b)

Fig. 5. Simulated S-parameters for the 1-D KFEBG microstrip structures of Fig. 1 to Fig. 3 with the dimensions of Table I. (a) S_{11}. (b) S_{21}.

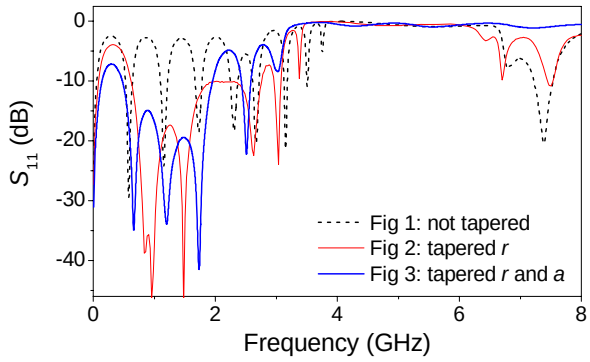

(a)

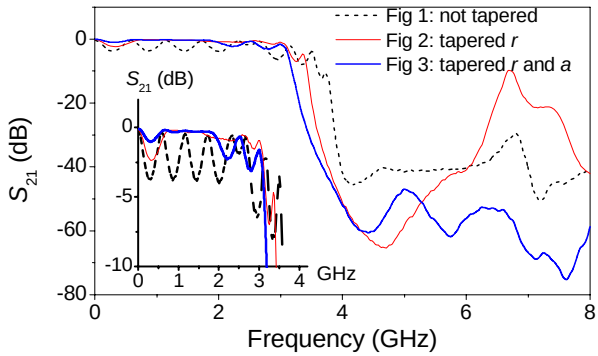

(b)

Fig. 6. Measured S-parameters for the 1-D KFEBG microstrip structures of Fig. 1 to Fig. 3 with the dimensions of Table I. (a) S_{11}. (b) S_{21}.

material with a dielectric constant $\varepsilon_r = 10.2$ ($\mathrm{tg}\delta = 0.0023$ at 10 GHz), substrate thickness h = 0.635 mm, and copper thickness t = 17.5 μm has been used as substrate for all 1-D KFEBG microstrip structures. The conductor strip has a width W = 0.594 mm, corresponding to a 50 Ω conventional microstrip line. The structures of Fig. 2 and Fig. 3 are conceived from the previous structure (Fig. 1) as described in the previous section, and the optimized dimensions are summarized in Table I.

Fig. 5 and Fig. 6 show, respectively, the simulated and measured S-parameters for the 1-D KFEBG microstrip structures of Fig. 1 to Fig. 3 with the dimensions of Table I. The simulations include the metallic and material losses. It can be seen that the pass-band that appeared between two rejection bands in previously published results with $r/a < 0.5$ is suppressed [9], [10]. A wide stop-band is achieved for $r/a = 0.55$, which can be useful for the design of antennas and other devices. Considering the losses in the connections, the non-idealities of the fabrication such as in the dimensions of the microstrip line and shape of the fractals (Fig. 4), and a slight difference of the dielectric constant with respect to the given value ($\varepsilon_r = 10.2$), the simulated and measured results present a reasonable agreement. In the case of the non-tapered structure (Fig. 1), the results in Figs. 5 and 6 present a high rejection level in the stop-band, but the pass-band has much ripple. This ripple is reduced by tapering the

Koch fractal dimensions in the periodic pattern with a Kaiser function (1), as described for the structure of Fig. 2. However, this has a negative side-effect in the rejection level of the stop-band, which becomes significantly narrower due to the decreasing *r*/*a* ratio along the periodic pattern. Hence, the width of the band-gap of the structure decreases, and the advantages of the Koch fractal pattern to obtain a compact wide band-gap structure partially disappear. However, the curves depicted in Figs. 5 and 6 for the structure of Fig. 3 show that wide band-gap characteristics can be restored by tapering not only the radius of the fractals but also the period or separation between them, producing the best results in terms of wide-band characteristics and ripple reduction among the three types of 1-D KFEBG designs considered in this work. Hence, high rejection level in a wide band-gap and low ripple in the pass-band are obtained by tapering the microstrip width and the Koch fractal dimensions in the top and bottom planes, respectively, with a Kaiser function and a varying period given by (3) with $C = 0.55$.

We have quantified the ripple reduction by evaluating the average of the oscillations of the measured S_{21} parameter from 300 kHz to 2.5 GHz. This average is, respectively, 2.98 dB, 1.36 dB and 0.81 dB for the structures of Figs. 1, 2 and 3. However, it can be seen that a small mismatch remains at low frequencies and cannot be completely removed by the tapering. This is in agreement with the application of the theory of small reflections to the calculation of the reflection coefficient to a tapered line [17].

In order to gain insight into any undesired effects due to coupling of radiated waves, we have analyzed the radiating characteristics as a function of frequency according to the relationship $1-|S_{11}|^2-|S_{21}|^2$ for the three simulated structures. The metallic and dielectric losses were considered lossless in order to isolate the undesired radiant effects. The average value of the radiation losses between 300 kHz and 8 GHz is 21.9 %, 15.4 % and 4.7 % for the structures of Fig. 1, Fig. 2 and Fig. 3, respectively. As it was expected, the structure of Fig. 1 is more radiant. The introduction of tapering techniques decreases considerably the radiation losses, producing the best results for the structure of Fig. 3. In addition, this design allows a reduction in size of approximately 20 % over the two other possibilities, as measured by the parameter *D* in Table I, giving as a result a compact wide-band KFEBG structure.

IV. Conclusion

In this paper, periodic patterns based on Koch fractal geometries have been applied to 1-D electromagnetic bandgap (EBG) microstrip structures. Moreover, the effects on the frequency response of a tapering of the dimensions and periodicity of the Koch fractal patterns with a Kaiser function are presented. The Koch fractal geometries allow conceiving 1-D Koch fractal electromagnetic band-gap (KFEBG) microstrip structures with *r*/*a* ratios higher than 0.5, which is the upper limit of the conventional 1-D EBG microstrip structure. As a result of exceeding this limit, the 1-D KFEBG microstrip structure achieves wide band-gap frequency characteristics. The ripple that appears in the pass-band is reduced by tapering the Koch fractal dimensions in the periodic pattern and the microstrip width with a Kaiser function, while the width of the bandgap is increased by modulating the fractal period with the same function. As a consequence of this, the size of the device is compacted.

References

[1] E. Yablonovitch, "Photonic band-gap structures," *Journal Opt. Soc. Amer B*, vol. 10, pp. 283-295, Feb. 1993.

[2] Y. Rahmat-Samii, and H. Mosallaei, "Electromagnetic band-gap structures: Classification, characterization and applications," in *Proc. Int. Conf. Antennas Propag.*, vol. 2, Manchester, Apr. 2001, pp. 560-564.

[3] H. Mosallei, and K. Sarabandi, "A compact wide-band EBG structure utilizing embedded resonant circuits", *IEEE Antennas Wireless Propag. Lett.* , vol. 4, pp. 5-8, 2005.

[4] L. Matekovits, G. C. Vietti Colomé, and M. Orefice, "Propagation of electromagnetic waves in a sinusoidaly modulated dielectric substrate", *IEEE Antennas Wireless Propag. Lett.*, vol. 6, pp. 207-210, 2007.

[5] J. Shibayama, R. Ando, J. Yamauchi, and H. Nakano, "An LOD-FDTD method for the analysis of periodic structures at normal incidence", *IEEE Antennas Wireless Propag. Lett.*, vol. 8, pp. 890-893, 2009.

[6] A. Della Villa, V. Galdi, F. Capolino, V. Piero, S. Enoch, and G. Tayeb, "A comparative study of representative categories of EBG dielectric quasi-crystals", *IEEE Antennas Wireless Propag. Lett.*, vol. 5, pp. 331-334, 2006.

[7] M. F. Karim, A. Liu, A. Yu, and A. Alpones, "Micromachined tunable filter using fractal electromagnetic bandgap (EBG) structures", *Sensors and Actuators A*, vol. 133, pp. 355-362, 2007.

[8] H. Hsu, M. J. Hill, R. W. Ziolkowski, and J. Papapolymerou, "A duroid-based planar EBG cavity resonator filter with improved quality factor", *IEEE Antennas Wireless Propag. Lett.*, vol. 1, pp. 67-70, 2002.

[9] V. Radisic, Y Qian, R. Coccili, and T. Itoh , "Novel 2-D photonic bandgap structure for microstrip lines," *IEEE Microwave Guided Wave Lett.*, vol. 8, pp. 69-71, Feb. 1998.

[10] T. Lopetegi, M. A. Laso, M. J. Erro, D. Benito, M. J. Garde, F. Falcone, and M. Sorolla, "Novel photonic bandgap microstrip structures using network topology," *Microw. Opt. Tech. Lett.*, vol. 25, pp. 33-36, Apr. 2000.

[11] T. Kim, and C. Seo, "A novel photonic bandgap structure for low-pass filter of wide stopband," *IEEE Microwave Guided Wave Lett.*, vol. 10 pp. 13-15, Jan. 2000.

[12] P. Kurgan, and M. Kitlinski, "Novel microstrip low-pass filters with fractal defected ground structures," *Microw. Opt. Tech. Lett.*, vol. 51, pp. 2473-2477, Oct. 2009.

[13] J. D. Ruiz, F. L. Martínez, and J. Hinojosa, "1-D Koch fractal electromagnetic bandgap microstrip structures with *r*/*a* ratios higher than 0.5," *Microw. Opt. Tech. Lett.*, vol. 53, pp. 646-649, Mar. 2011.

[14] C. Puente-Baliarda, J. Romeu, and A. Cardama, "The Koch monopole: A small fractal antenna," *IEEE Trans. Antennas Propagat.*, vol. 48, pp. 1773-1781, Nov. 2000.

[15] K. J. Vinoy, J. K. Abraham, and V. K. Varadan, "On the relationship between fractal dimension and the performance of multi-resonant dipole antennas using Koch curves", *IEEE Trans. Antennas Propag.*, vol. 51, pp. 2296-2302, Sep. 2003.

[16] M. A. G. Laso, M. J. Erro, T. Lopetegui, D. Benito, M. J. Garde and M. Sorolla, "Optimization of tapered Bragg reflectors in microstip technology," *International Journal of Infrared and Milimeter Waves*, vol. 21, pp. 231-245, Feb. 2000.

[17] D. M. Pozar, *Microwave Engineering*. New York: Wiley, 1998.